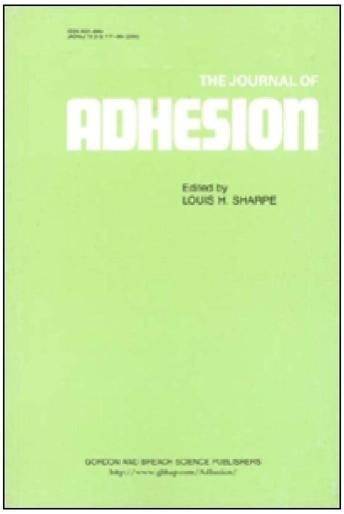

The Journal of Adhesion
Publication details, including instructions for authors and subscription information:
http://www.informaworld.com/smpp/title~content=t713453635

The Influence of Ti-6AI-4V Chromic Acid Anodization Conditions Upon Anodic Oxide Thickness and Topography

J. A. Skilest[a]; J. P. Wightman[a]
[a] Center for Adhesion Science, Department of Chemistry, Virginia Polytechnic Institute and State University, Blacksburg, Virginia, U.S.A.

To cite this Article Skilest, J. A. and Wightman, J. P.(1988) 'The Influence of Ti-6AI-4V Chromic Acid Anodization Conditions Upon Anodic Oxide Thickness and Topography', The Journal of Adhesion, 26: 4, 301 — 314
To link to this Article: DOI: 10.1080/00218468808071293
URL: http://dx.doi.org/10.1080/00218468808071293

J. Adhesion, 1988, Vol. 26, pp. 301–314
Reprints available directly from the publisher
Photocopying permitted by license only

Printed in the United Kingdom

The Influence of Ti–6Al–4V Chromic Acid Anodization Conditions Upon Anodic Oxide Thickness and Topography†

J. A. SKILES‡ and J. P. WIGHTMAN

Center for Adhesion Science, Department of Chemistry, Virginia Polytechnic Institute and State University, Blacksburg, Virginia 24061, U.S.A.

(Received November 21, 1987; in final form June 6, 1988)

Chromic acid (CA) anodization of Ti–6Al–4V (6% Al, 4% V by weight) produced an anodic oxide on the alloy surface. The influence of specific CA anodization conditions upon anodic oxide thickness was determined. Each CA anodization condition tested was defined by setting five variables: (1) solution composition; (2) anodization time; (3) solution temperature; (4) initial current density; and, (5) anodization potential.

The results confirmed observations by previous workers about oxide thickness and structure. Data indicated an inverse relationship between film thickness and temperature, and that film growth rate decreases with time.

KEY WORDS Ti-6Al-4V; chromic acid anodization; oxide thickness; oxide topography; oxide morphology.

INTRODUCTION

In general terms, the strength and durability of metal/adhesive bonds depend on the following factors: (1) the inherent strength

---

† Based in part on Ph.D. dissertation of J. A. Skiles.

‡ Present address: Aluminum Company of America, Alcoa Technical Center, Alcoa Center, Pennsylvania 15069, U.S.A.

and durability of the materials to be joined; (2) bonding conditions; (3) the bond design, and; (4) bulk and surface properties of both the metal and the adhesive, which are influenced by bulk processing and by metal and adhesive prebond treatments. It is desirable to identify and to understand how all of these variables interrelate and affect metal/adhesive bond strength and durability for specific materials and envirommental conditions, in order to produce reliably strong and durable metal/adhesive bonds for both structural and non-structural applications. Much of the present defense, industrial, and aircraft technology dictates that an adhesive, rather than a mechanical fastener, join similar metals, or join a metal to a dissimilar material. The dissimilar material may be another metal, an unfilled or inorganic particle filled polymer, or a composite.

Ti-6Al-4V is considered to be a good choice for structural metal/adhesive bonds. Titanium alloys have a strength/weight ratio 50% higher than stainless or alloy steels. In addition to good strength-to-weight characteristics, Ti–6Al–4V has corrosion resistance to salt water and many acid and alkaline solutions.

CA anodization of Ti–6Al–4V is an acceptable prebond treatment to produce a durable, porous oxide on the surface.[1–4] The porosity is considered to be beneficial to adhesive bonding in that the surface area for physical and/or chemical bonding of the adhesive to the oxide is increased. Oxide microroughness, or protrusions above the pore cells with dimensions $\leq 0.1\,\mu m$, are considered to provide a high degree of mechanical interlock of the oxide to the adhesive.[2–4]

This work described herein related Ti-6A1-4V CA anodization conditions to the resulting anodic oxide thickness. Each condition is described by setting five variables: (1) solution composition; (2) solution temperature; (3) anodization time; (4) initial current density; and (5) anodization potential. Anodic oxide morphology was determined for one, and oxide topography was determined for two anodization conditions.

This work was conducted to provide a better understanding of the effects of anodization conditions upon anodic oxide characteristics. Such information can be used to evaluate and select an anodic oxide with the appropriate characteristics to contribute to the strength and durability of an anodized Ti–6A1–4V/adhesive bond.

EXPERIMENTAL

A. Chromic acid anodization methods and materials

Ti–6Al–4V coupons, 152.4 mm × 25.4 mm × 1.3 mm, were anodized and used in multiple beam interferometry (MBI) studies. The coupons were provided by personnel at the NASA-Langley Research Center. A 38.1 μm thick Ti–6Al–4V foil was anodized for the transmission electron microscopy (TEM) and selected area electron diffraction (SAED) studies. The foil was purchased from Arnold Subsidiary Magnetics and Electronics, Inc.

The Ti–6Al–4V was cleaned before anodization as described in Table I. A glass bead blast was used to clean the metal surface. The metal was then exposed to a sodium hydroxide solution to remove inorganics, and subsequently acid etched to remove the natural oxide from the surface.

Immediately after the preanodization cleaning treatment, the surface was anodized in a 5% CA solution at pH 0.5. Technical grade chromium trioxide and distilled, deionized water were used to make the solution. A 49% hydrofluoric acid (HF) solution was added to the CA solution at the beginning of all but one of the anodizations.

During anodization, Ti–6Al–4V was used both as the anode and the cathode, and a 0.5 A, constant voltage power supply was used. Air agitation of the solution was used to insure uniform anodization on both sides of the anode.

TABLE I
Procedure for Ti–6Al–4V preanodization treatment

1. Glass bead blast coupons with medium size Ferro glass beads.
2. Immerse 5 minutes in a 343 K, 5% NaOH solution (500 ml of solution for 6 coupons).
3. Rinse in distilled, deionized water.
4. Immerse 5 minutes in 500 ml distilled, deionized water.
5. Repeat Step 4.
6. Pickle at 298 K for 5 minutes in a deionized water solution containing 15% by volume of 70% HNO_3, and 3% by volume of 49% HF (100 ml of solution for 6 coupons). Pickle a 55 mm long × 25 mm wide area.
7. Repeat Steps #4 and #5.
8. Nitrogen dry.

Note: Coupons were anodized immediately after preanodization treatment.

The eight anodization conditions tested in this study are described in Table II. The initial current density was based upon the geometric surface area of the coupons.

After anodization, the coupons were cleaned to remove any residual solution. The post-anodization cleaning method is described in Table III.

B. MBI anodic oxide thickness measurement method

MBI was used to measure anodic oxide thickness for the anodized Ti–6Al–4V. Figure 1 is a schematic diagram of the interferometric setup. Monochromatic light at 632.8 nm from a He–Ne laser was attenuated and collimated. It was then reflected off the substrate and a coated reference mirror which was parallel to the Ti–6Al–4V surface. Constructive and destructive interference of light reflected from the surface produced alternating light and dark fringes. The anodic oxide thickness, n, is given by:

$$n = (a/b)(\lambda/2) \qquad (1)$$

where λ is 632.8 nm, and a and b are measurements of fringe spacings.

Figure 2 is an interferogram at 28.4× magnification used to measure the anodic oxide thickness. The actual area photographed was 7.6 mm × 5.0 mm. The alternating fringes from the unanodized Ti–6Al–4V connect to the alternating fringes from the anodic oxide. The fringe curvature occurs in the anodic oxide/unanodized Ti–6Al–4V transition region, which spans a length of approximately 0.1 cm.

These curved, alternating bright and dark fringes in the transition region are important to determine the exact anodic oxide thickness. The interconnecting fringe pattern allows anodic oxide thicknesses $\geq \lambda/2$ to be determined from the interferometric pattern.

We note that, for these MBI measurements, the anodic oxide was produced on a polished Ti–6Al–4V substrate to minimize fringe curvature. Also, approximately 70 nm of silver was evaporated onto the Ti–6Al–4V substrate to increase the reflectivity of the surfaces for MBI measurements.

TABLE II
Chromic acid anodization conditions for Ti–6Al–4V

Anodization variable	Anodization condition							
	#1	#2	#3	#4	#5	#6	#7	#8
Solution composition	CA/HF	CA/HF	CA/HF	CA/HF	CA/HF	CA/HF	CA/HF	CA
Time (min)	20	20	20	20	20	20	60	20
Voltage (V)	10	10	10	10	10	10	10	39
Solution temperature (±2 K)	298	298	298	283	283	278	298	298
Initial current density (±2 A/m^2)	20	30	54	20	30	30	30	30

TABLE III
Post-anodization Ti-6Al-4V cleaning method

1. Soak Ti-6Al-4V coupons in a 500 ml volume distilled, deionized water 2 minutes.
2. Repeat Step 1.
3. Soak Ti-6Al-4V coupons in a clean 500 ml volume of distilled, deionized water 15 minutes.
4. Repeat Steps #1 and #2.
5. Nitrogen dry anodized coupons. .

Note: This procedure is used for cleaning six coupons simultaneously. The coupons were immersed so as to clean the 25.4 square mm of anodized surface area.

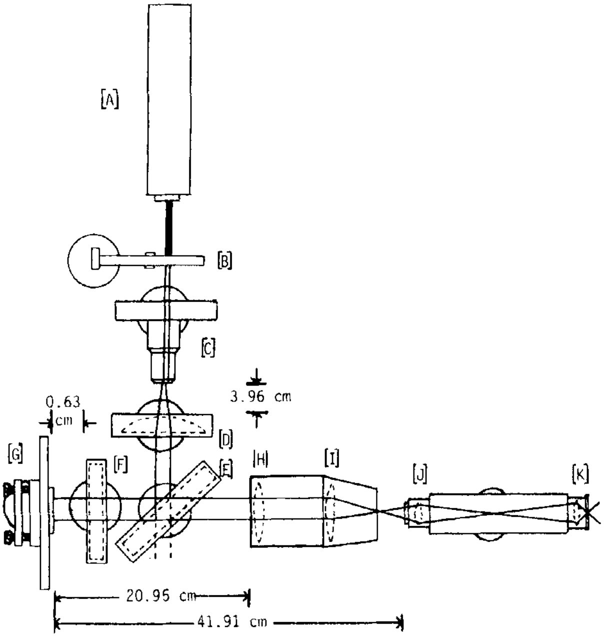

FIGURE 1 Interferometer schematic diagram. [A] He-Ne laser, Class III B, 40 mW; [B] Attenuator; [C] Objective lens; [D] Condenser lens; [E] Beam splitter; [F] Coated mirror—70% transmission, 30% reflection; [G] Sample on tilt stage; [H] Binocular lens—1×; [I] Binocular lens—1×; [J] Microscope lens—4.5×; [K] Microscope lens 7×.

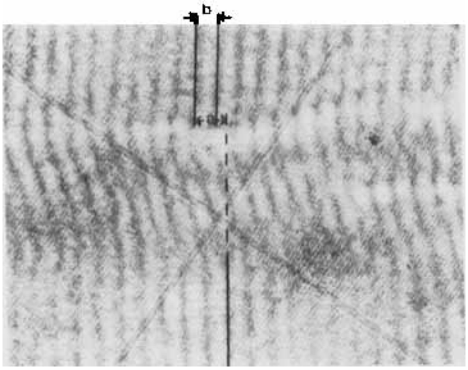

FIGURE 2 Interferogram of fringe pattern used to measure Ti–6Al–4V anodic oxide thickness (28.4×).

C. TEM and SAED

TEM analyses were conducted for the anodic oxide produced by conditions #1 or #4 described in Table II, and SAED analyses were conducted for the anodic oxide produced per anodization condition #4. Both were conducted at Structure Probe, Inc. (West Chester, Pennsylvania), using a JEOL 100CX TEM at a 100 kV accelerating voltage.

The preparation of specimens for TEM and SAED analyses included gold sputtering, embedding in epoxy and microtoming the foil to produce cross sections or parallel sections which were approximately 60 to 80 mm thick. TEM analyses of the cross sectioned oxide elucidated oxide roughness, topography and thickness; parallel sections of the oxide elucidated oxide topography. Parallel sections were analyzed by SAED to determine oxide morphology from diffraction.

D. SEM

A JEOL JSM-36C scanning electron microscope was used to characterize the oxide topography for condition #2 in Table II. A 9.5 mm diameter sample, which was punched from the anodized titanium alloy and gold coated, was used in this analysis.

RESULTS AND DISCUSSION

A. Anodic oxide structure and topography

SAED analysis of an anodic oxide in cross section indicated that the oxide was primarily amorphous. Figures 3 and 4 are TEM photomicrographs through parallel sections of the oxides. The oxide pore diameter and wall thickness were similar for both the 283 K and 298 K anodization solution temperature. For both oxides, pore diameters of 25 to 40 nm with a wall thickness of approximately 10 nm were measured.

Figures 5 and 6 are TEM photomicrographs of the cross sectioned oxide. Regular, columnar pore structures are evident in both. A thin barrier oxide layer, approximately 15 nm thick, is apparent at the oxide base. For both oxides examined, the oxide has a peak-to-valley roughness of approximately 170 nm and follows the metal substrate contours.

The hydrofluoric acid added to the CA anodization solution influences oxide composition and is important to oxide pore formation. Clearfield, Shaffer and Ahearn[5] have determined that the fluorine concentration is greater in the barrier layer than in the

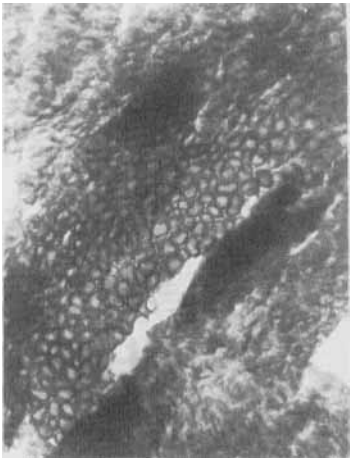

FIGURE 3. Transmission electron photomicrograph of a parallel section of an anodic oxide produced by 20 min CA/HF anodization at: 283 K, 20 A/m^2, and 10 V (200,000×).

FIGURE 4. Transmission electron photomicrograph of a parallel section of an anodic oxide produced by 20 min CA/HF anodization at: 298 K, 20 A/m^2, and 10 V (200,000×).

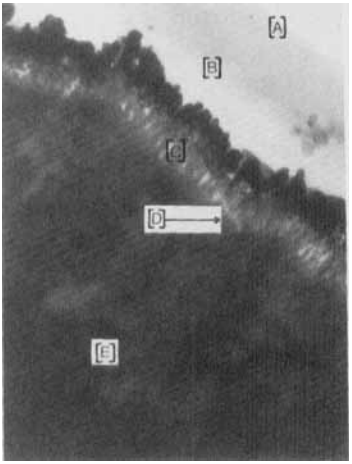

FIGURE 5. Trnasmission electron photomicrograph of a cross section of an anodic oxide produced by 20 min CA/HF anodization at: 283 K, 20 A/m^2, and 10 V (200,000×). [A] epoxy mount; [B] Gold deposit; [C] Oxide; [D] Oxide barrier layer; [E] Ti–6Al–4V substrate.

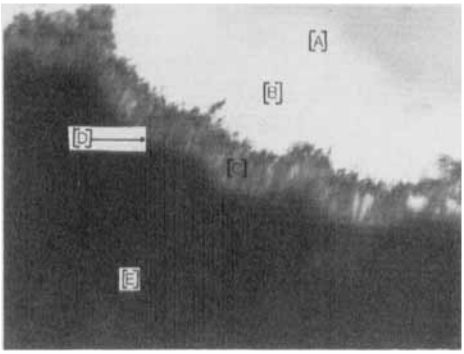

FIGURE 6 Transmission electron photomicrograph of a cross section of an anodic oxide produced by 20 min CA/HF anodization at: 298 K, 20 A/m^2, and 10 V (200,000×). [A] Epoxy mount; [B] Gold deposit; [C] Oxide; [D] Oxide barrier layer; [E] Ti–6Al–4V substrate.

more porous oxide for this titanium alloy. Cheng[6] reported that pores were present on the anodic oxide only when HF was added to the chromic acid solution to control the current density. A smooth, compact oxide was obtained when HF was not added.

Figure 7 is a SEM photomicrograph of Ti–6Al–4V after CA/HF anodization by condition #2 in Table II. Irregularly shaped and nonuniformly distributed structures, which are approximately 2 μm wide and 3 μm long, are apparent on the anodized surface. Similar structures have been observed by Hendricks[7] for phosphoric acid anodized Ti–6Al–4V preceded by a nitric acid/hydrofluoric acid pickle. Hendricks referred to these structures as etch pits.

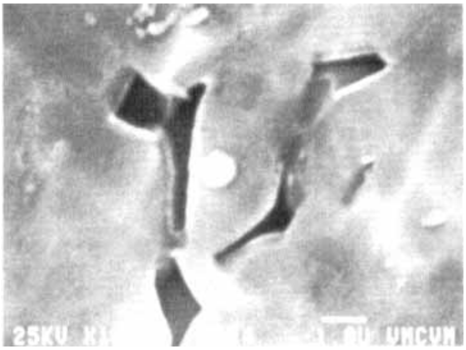

FIGURE 7 Scanning electron photomicrograph of the Ti–6Al–4V surface after preanodization treatment and CA/HF anodization (10,000×).

B. Oxide thicknesses

a. A comparison of TEM and MBI oxide thickness measurements Two direct methods were used to measure oxide thickness: TEM photomicrographs of the oxide in cross section at a nominal magnification of 200,000×, and MBI photographs at 28×. Eight to ten MBI interference shift measurements or TEM measurements were made to obtain the average anodic oxide thickness and range. The results are summarized in Table IV.

Regarding condition #4 in Table II, for example, there was good agreement between the MBI and TEM oxide thickness results, as shown in Table IV. The average oxide thickness was 120 nm based upon TEM measurements and 160 nm based upon MBI measurements. The variation in the two measurements is attributed to the variation in the oxide thickness across a given surface and/or variation between two coupons anodized simultaneously in the same solution.

MBI was the primary method used to measure oxide thickness as a function of anodization condition because the interferometer was more readily accessible and had lower operating costs than the TEM.

b. Influence of anodization solution composition upon oxide thickness A thin (20 nm) oxide was formed on the Ti–6Al–4V surface when the surface was chromic acid anodized without hydrofluoric acid. However, this oxide was thinner than any of the CA/HF anodic oxides reported in Table IV.

c. Influence of CA/HF anodization time upon oxide thickness Increasing the CA/HF anodization time from 20 to 60 minutes approximately doubled the average oxide thickness, from 140 to 290 nm, as shown in Table IV.

d. Influence of CA/HF anodization solution temperature and initial current density upon oxide thickness Oxide thickness is not dependent upon initial current density for the 20 min, 10 V Ti–6Al–4V anodization conditions examined, as evident in Table IV. There is a nonlinear, inverse relationship between oxide thickness and solution temperature.

TABLE IV
Chromic acid anodized Ti-6Al-4V oxide thickness data

Oxide thickness data	Anodization condition							
	#1	#2	#3	#4	#5	#6	#7	#8
Average thickness								
MBI	NM[1]	140	110	160	410	460	290	20
TEM	80	NM	NM	120	NM	NM	NM	NM
Thickness range								
MBI	NM	120–160	90–140	150–180	390–440	430–500	250–300	10–40
TEM	65–85	NM	NM	95–150	NM	NM	NM	NM

[1] NM-Not measured.

As shown in Table IV, average oxide thickness increased by approximately a factor of 3, from 140 nm to 410 nm, when the solution temperature was decreased from 298 K to 283 K at a 30 A/m^2 initial current density. However, the oxide thickness was not significantly changed when the solution temperature was further rediced to 278 K.

A similar trend was observed at an initial current density of 20 A/m^2. The average oxide thickness increased by a factor of 2 when the solution temperature was 283 K rather than 298 K.

For a solution temperature of 298 K, average oxide thickness increased by approximately a factor of 2 when the initial current density was increased from 20 to 30 A/m^2. However, a further increase in initial current density from 30 to 54 A/m^2 did not significantly affect oxide thickness.

Table IV also shows that an oxide thickness was not unique for a set of CA/HF anodization conditions. An average oxide thickness of 140 nm was produced at a CA/HF anodization condition of: 20 min, 10 V, 30 A/m^2, and 298 K. Approximately the same average oxide thickness, 160 nm, was produced at: 20 min, 10 V, 20 A/m^2, and 283 K. While the rate of oxide formation and dissolution may have differed for these two anodization conditions since the initial current density and solution temperature differed, apparently the net effect upon oxide thickness was the same.

SUMMARY

There was no relationship between oxide thickness and initial current density. CA/HF anodizing conditions tested produced thicker oxides than did CA anodization conditions tested. An inverse, nonlinear relationship was noted between oxide thickness and anodization solution temperature. An increase in anodization time from 20 to 60 minutes, holding all other anodization variables constant, doubled anodic oxide thickness.

CA/HF anodization of Ti–6Al–4V produced an anodic oxide which was amorphous and followed the contours of the Ti–6Al–4V substrate. The peak-to-valley roughness was about 170 nm, and regular, columnar pores were present with diameters of 25 to 40 nm and a wall thickness of about 10 nm.

Anodization without HF produced an average oxide thickness of only 20 nm. This represents a sevenfold decrease in average oxide thickness, compared to anodization with HF.

Acknowledgements

This work was supported by the Office of Naval Research. Optical table and laser were provided by Poly-Scientific, Litton Industries, Inc.

References

1. Y. Moji and J. A. Marceau, U.S. Patent No. 3,959,091 The Boeing Company, (1976).
2. B. M. Ditchek, K. R. Breen, T. S. Sun and J. D. Venables, *25th Nat. SAMPE Symp. and Exhibition,* 13 (1980).
3. B. M. Ditchek, K. R. Breen, T. S. Sun and J. D. Venables, *12th Nat. SAMPE Tech. Conf.*, 882 (1980).
4. M. Natan, J. D. Venables and K. R. Breen, *27th Nat. SAMPE Symposium*, 178 (1982).
5. H. M. Clearfield, D. K. Shaffer and J. S. Ahearn, *18 Int. SAMPE Tech. Conf.*, 921 (1986).
6. A. Cheng, "Anodic Oxide Formation of Ti-6Al-4V in Chromic Acid for Adhesive Bonding" M.S. Thesis, Virginia Polytechnic Institute and State University (1983).
7. C. L. Hendricks, The Boeing Aerospace Company Contract Report #NAS1-15605, prepared for the National Aeronautics and Space Administration, (1980).